Magnetic vortex crystal formation in the antidot complement of square artificial spin ice

C. I. L. de Araujo,[1,a)] R. C. Silva,[1] I. R. B. Ribeiro,[1] F. S. Nascimento,[1] J. F. Felix,[1] S. O. Ferreira,[1] L. A. S. Mól,[2] W. A. Moura-Melo,[1] and A. R. Pereira[1]
[1]*Departamento de Física, Universidade Federal de Viçosa, Viçosa 36570-900, Minas Gerais, Brazil*
[2]*Departamento de Física, ICEx, Universidade Federal de Minas Gerais, Belo Horizonte 31270-901, Minas Gerais, Brazil*

(Received 4 December 2013; accepted 20 February 2014; published online 4 March 2014)

We have studied ferromagnetic nickel thin films patterned with square lattices of elongated antidots that are negative analogues of square artificial spin ice. Micromagnetic simulations and direct current magnetic moment measurements reveal in-plane anisotropy of the magnetic hysteresis loops, and the formation of a dense array of magnetic vortices with random polarization and chirality. These multiply-connected antidot arrays could be superior to lattices of disconnected nanodisks for investigations of vortex switching by applied electric current. © *2014 AIP Publishing LLC*. [http://dx.doi.org/10.1063/1.4867530]

Nowadays, nanomagnetism is one of the most exciting branches of basic and applied research. Several applications have become reality and many others are under way. The experimental advances to fabricate and characterize nanosamples have provided a lot of exciting magnetic phenomena and possibilities at such a scale. For instance, magnetic thin films with nanometers thicknesses display peculiar magnetization patterns depending on their shapes. For instance, a thin nanodisk may support a single topological vortex-like configuration, while Landau vortex-type states show up in square/rectangular nanosamples. On the other hand, elongated shapes like narrow cylinders and ellipsoids generally exhibit single-domain patterns with strong Ising-like anisotropy along the major dimension (see Refs. 1 and 2 for reviews). Holes (also called antidots) can also be intentionally introduced in such magnetic nanomaterials, and their influences on the vortex structure and dynamics have been intensively investigated, mainly in magnetic nanodisks.[3–7] With all advances in nanomagnetism, many technological applications of topological objects such as vortices and skyrmions were raised, including magnetic logic and storage[7,8] with promising relevance in spintronics, magneto-mechanical apoptosis reactivation in cancer cells,[9] among many others.

Elongated ferromagnetic nanoislands organized in suitable two-dimensional (2*D*) arrangements have also deserved great attention. Actually, in such artificially structured arrays, the ice rule and geometrical frustration are present so that they bear residual entropy even at zero temperature, similar to what occur to the water ice. For this resemblance with water ice, those systems have been named artificial spin ices (ASI).[10] The realization of artificial ice systems has also been successfully applied to other compounds such as colloidal systems[11] and superconducting antidots.[12,13] Among several interesting properties, ASI were predicted[14–16] to support emergent magnetic monopole excitations interacting via a Coulomb potential, similar to that already observed in natural three-dimensional (3*D*) spin ice crystals.[17–21] However, in 2*D*-ASI, the north and south poles are connected by an additional energetic string,[16] developing into a structure similar to a pair of Nambu monopoles.[22,23] These predictions were soon confirmed by experiments.[24] Such findings shed light into the real possibilities of using isolated magnetic poles as the physical carriers of charge, energy, and momentum—a kind of electricity with magnetic charges, the so called magnetricity. In order to decrease the string tension and provide monopoles separation inside artificial spin ice samples, different geometries and insertion of defects (like non-uniformity or dislocation of the cell sizes) have been proposed.[23]

In turn, the insertion of nanometric antidots in continuous thin films is a timely topic in the frontier of basic and applied research. Antidots may be displayed in regular geometrical arrangements depicting a number of patterns as diamond-type, square, triangular, and so on.[25–27] The main results of these works are the changes observed in the demagnetization field and domain wall pinning, which bring about the emergence of magnetic anisotropy in the patterned thin films as well as a huge increase in the coercive field. Such a behavior strongly suggests antidots systems as promising structures for application in high-density magnetic storage, predicted to be around 0.1 Tb/cm^2 and reading/writing velocity (0.5 Gbs^{-1}).[28,29]

Here, we report on the experimental fabrication and theoretical study of a structure composed by a lattice of antidots (elongated holes), resembling the geometrical arrangement of nanoislands in a square ASI, as shown in Fig. 1. This system (here referred to as antidot-ASI) was built as follows: on the silicon (110) substrate with area of 1 cm^2, previously cleaned by Radio Corporation of America (RCA) process, a 200 nm Polymethylmethacrylate (PMMA) layer was deposited by spin coating at 4000 rpm during 40 s. The PMMA (dried for 10 min in hotplate at 120 °C) has 1 nm root mean square (RMS) roughness measured by atomic force microscopy. The sample was carried into the RAITH *e_LINE* plus system chamber, where the exposure of the antidot design was performed. Such design was repeated a thousand times to form 1 mm^2 lithographed area. The parameters utilized were beam acceleration of 20 kV and area cleaning dose of

a)Electronic mail: dearaujo@ufv.br

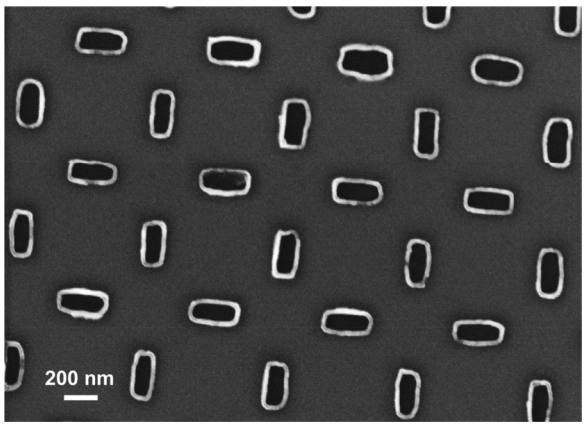

FIG. 1. SEM–FEG micrography of the antidot lattice sample (here referred to as antidot-ASI) composed by 25 nm Ni thin film (grey). The antidots are the black holes and their array mimics the artificial spin ice geometry.

160 C/cm^2. After the PMMA developing, the samples were placed into the Thermionics *E_Beam* evaporation system where a 25 nm nickel (Ni) film was evaporated over a 8 nm titanium seed layer (used to increase the adhesion). A cap layer of 3 nm gold was evaporated over the sample to prevent the Ni oxidation. Finally, the structures were defined by lift-off process in acetone ultrasonic bath. The final sample structures were investigated by scanning electron microscopy with field emission gun (SEM–FEG). In order to study the influence of our patterned antidot-ASI on the thin film hysteresis loop, some magnetic characterizations were realized in a Microsense *EV*9 vibrating sample magnetometer (VSM). The total magnetization of the samples was taken in configurations with external magnetic field applied along 0° and 45° in relation to the antidot lattice horizontal side. In Fig. 1, we present the SEM–FEG image of the final sample where the Ni thin film is represented by the grey color and the antidots by black elongated holes.

VSM measurements in an antidot-ASI (see Fig. 2(a)) show the square-like shape of the hysteresis loop and an increase of the coercive field when the external magnetic field ($\vec{H}$) is applied along the diagonal (45°) when compared with the results obtained for a field applied at 0°.

Now, we theoretically describe the main characteristics of the system which should be responsible for the observed behaviors of the hysteresis. In order to investigate the spin configurations in different stages of the hysteresis curve (with field applied at both 0° and 45°), micromagnetic simulations were performed with computational codes provided by the Object Oriented MicroMagnetic Framework (OOMMF),[30] which are based upon the Landau-Lifshitz-Gilbert (LLG) equation[31,32] and effectively describes magnetization ($\vec{M}$) dynamics

$$\frac{\partial \vec{M}}{\partial t} = -\gamma \vec{M} \times \vec{H}_{eff} + \frac{\alpha}{M_s} \vec{M} \times \frac{\partial \vec{M}}{\partial t}, \qquad (1)$$

where γ is the gyromagnetic ratio, M_s is the saturation magnetization, while H_{eff} accounts for the effective magnetic field (composed by the external magnetic field, the magnetocrystalline anisotropies, and the dipolar and exchange interactions). Equation (1) is used to determine the minimum

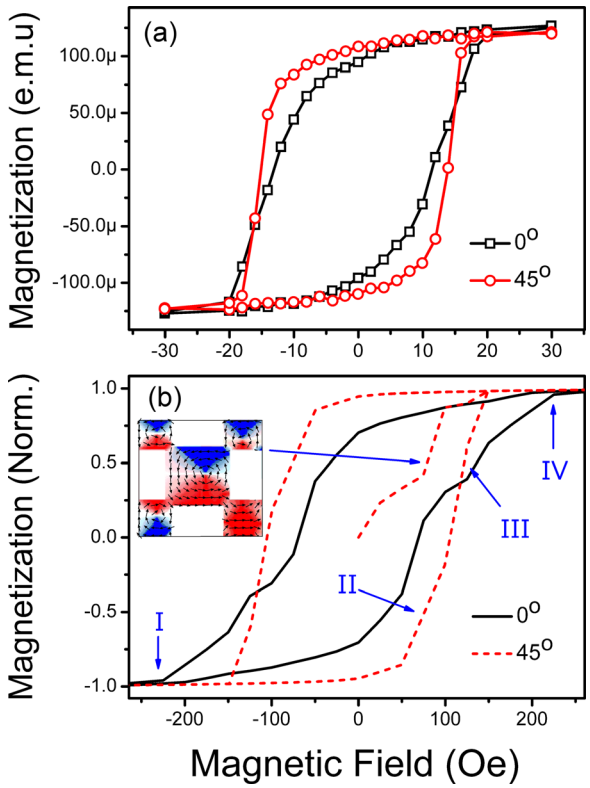

FIG. 2. (a) Magnetization curves obtained by VSM with field oriented at 0° and 45° in respect to the antidot lattice side. (b) Hysteresis loop from the micromagnetic simulation, where the Roman numeral labels represent the position of each magnetization map showed in Fig. 3. The inset shows the vortex configuration in the beginning of the hysteresis curve.

energy and the transitions between spin configurations. The simulation parameters adopted for Ni are the exchange (stiffness) constant $A^{Ni} = 9 \times 10^{-12}$ J/m and saturation magnetization $M_s = 4.3 \times 10^5$ A/m. The structures were divided in cubic meshes with side size $l = 5$ nm, which are smaller than Ni exchange length ($l_{ex} = \sqrt{A/4\pi M_s^2} \approx 7.72$ nm). The hysteresis loop obtained by simulation is shown in Fig. 2(b), and it is in good qualitative agreement with our experimental measurements. However, the theoretical field range is much higher than that of the experimental results. These quantitative differences come about mainly for two reasons: First, OOMMF is a zero temperature code and the experiments were performed at room temperature; second, for saving computational efforts, the simulations have been performed by taking into account only a small portion of the whole system (without the continuous border film, around $3 \times 3\ \mu m^2$), while our experimental measurements consider the whole sample. It is a good indication that the sample should be patterned for possible applications in magnetic storage. In our case, only 1 mm^2 from the 1 cm^2 of the sample was patterned and so the coercivity in the experimental hysteresis loop has a huge influence of the temperature and of the large area of non-patterned Ni thin film, as well. However, the qualitative agreement between experimental and theoretical anisotropy indicates that the film border shape does not affect the results, except when the field range decreases.

From the magnetic configuration in each range of the hysteresis loop obtained by simulations (see Fig. 3), it may be realized that the spins are parallel to the system border

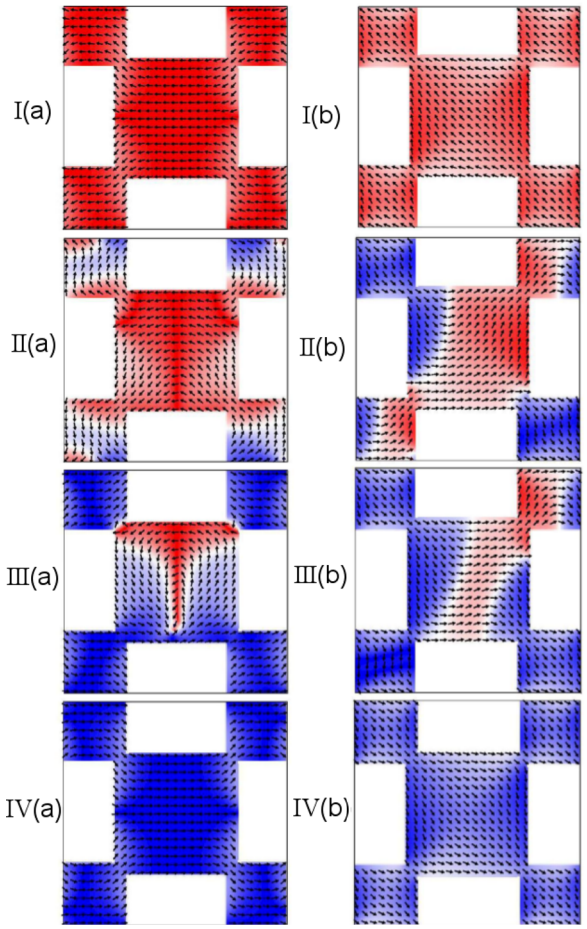

FIG. 3. Micromagnetic analysis of magnetization dynamics in one cell during the hysteresis simulation, see Fig. 2. For (a)-panels, the field is applied at 0°, while for (b)-panels, $\vec{H}$ lies along 45°. The red and blue areas represent the spins saturated to negative and positive fields, respectively.

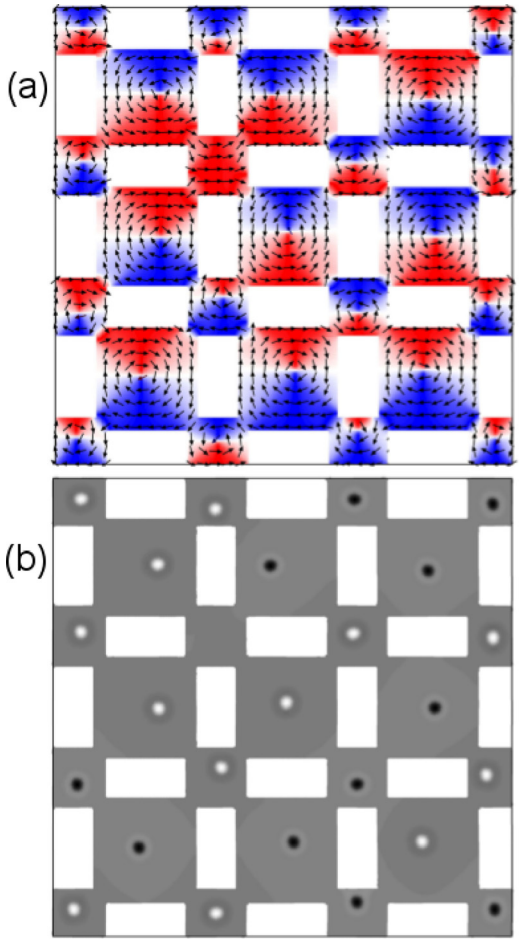

FIG. 4. Results from simulation of 9 cells showing the vortex-crystal chiralities (panel (a)) and core polarizations (black and white central spots, panel (b)). It is noteworthy to mention the random distribution of both quantities throughout the sample.

(this reduces magnetostatic energy). Thus, in the square geometry, when the magnetic field is applied along the sides of the cells (Fig. 3(a), I–IV), the influence of the pinned domains (in the antidot cells sides) perpendicular to the field yields a small contribution to the pinning process and a high field is necessary for the total magnetic saturation. When the field is applied along the diagonal of the cells (Fig. 3(b), I–IV), both pinned domains give comparable contributions for the square-like shape and increase of the coercivity in the hysteresis loop, which is in agreement with our experimental observation.

Whenever analyzing the magnetization behavior during spins relaxation in the very beginning of the hysteresis curve (inset of Fig. 2(b)), we realize the appearance of vortex-crystal patterns throughout the sample, similarly to what happens to the more diluted vortex structures in ferromagnetic antidot lattices previously studied by Bhat *et al.*[33] The vortex-crystal is presented in Fig. 4(a). Note that the vortex chiralities follow a random distribution. Our simulations indicate that the vortex-crystal appears only when the Ni thickness is larger than 25 nm. Since the expected Curie temperature T_c for this thickness is close to the bulk value ($T = 631$ K (Ref. 34)), this vortex-crystal configuration could be observed even above room temperature. The spins near the vortex centers become out of plane (up or down polarization) in order to minimize the magnetostatic energy. Figure 4(b) illustrates the polarizations of the vortex-crystal obtained by simulation. The black and white dots represent opposite vortex core polarizations which are randomly distributed throughout the pattern. Some phenomena concerning these structures in an antidot-ASI can be explored; as examples, Koyama *et al.*[35] have shown the possibility of aligning every vortex in an array of nanodisks with the same polarity and chirality by applying constant magnetic field perpendicular to the sample. In addition, alternating electric current can be used to achieve vortex switching, as suggested by Kasai *et al.*[36]

In summary, we have nanofabricated an antidot lattice (antidot-ASI) on Ni thin film in which the antidots are elongated holes (ellipse-like) displayed in an arrangement, which resemble the magnetic nanoislands in an artificial square spin ice. Our experimental results show an increase in the coercivity and squareness of the hysteresis loop, and these behaviors were qualitatively confirmed by micromagnetic simulations. Previously, similar behaviors have already been observed in other antidot systems.[37] One of the most important results presented here is the role of the proposed geometry in the formation of a topological crystal of vortices in the ferromagnetic thin film. These vortices may induce several interesting properties in the system. For instance, the possibility of creation, manipulation, and maintenance of such

vortex-crystal in an electrically connected sample at room temperature could be very useful for future applications in spintronics.

The authors are grateful to P. R. Soledade and J. P. Sinnecker (LABNANO/CBPF-Brazil) for technical support during electron microscopy/nanolithography work and to Professor A. A. Pasa (UFSC-Brasil) for the utilization of LFFS and LMCMM facilities. They also thank CAPES, CNPq, and FAPEMIG (Brazilian agencies) for partial financial support.

[1]*Spin Dynamics in Confined Magnetic Structures I*, edited by B. Hillebrands and K. Ounadjela (Springer, 2002), Vols. 1–3.
[2]*Nanomagnetism: Ultrathin Films, Multilayers and Nanostructures*, edited by D. L. Mills and J. A. C. Bland (Elsevier, 2006).
[3]M. Rahm, J. Biberger, V. Umansky, and D. Weiss, J. Appl. Phys. **93**, 7429 (2003).
[4]A. R. Pereira, J. Appl. Phys. **97**, 094303 (2005).
[5]R. L. Silva, A. R. Pereira, R. C. Silva, W. A. Moura-Melo, N. M. Oliveira-Neto, S. A. Leonel, and P. Z. Coura, Phys. Rev. B **78**, 054423 (2008).
[6]W. A. Moura-Melo, A. R. Pereira, R. L. Silva, and N. M. Oliveira-Neto, J. App. Phys. **103**, 124306 (2008).
[7]M. Rahm, J. Stah, and D. Weiss, Appl. Phys. Lett. **87**, 182107 (2005).
[8]J. Iwasaki, M. Mochizuki, and N. Nagaosa, Nat. Nanotechnol. **8**, 742 (2013).
[9]D.-H. Kim, E. A. Rozhkova, I. V. Ulasov, S. D. Bader, T. Rajh, M. S. Lesniak, and V. Novosad, Nature Mater. **9**, 165 (2010).
[10]R. F. Wang, C. Nisoli, R. S. Freitas, J. Li, W. McConville, B. J. Cooley, M. S. Lund, N. Samarth, C. Leighton, V. H. Crespi, and P. Schiffer, Nature **439**, 303 (2006).
[11]C. J. O. Reichhardt, A. Libsal, and C. Reichhardt, New J. Phys. **14**, 025006 (2012).
[12]M. L. Latimer, G. R. Berdiyorov, Z. L. Xiao, F. M. Peeters, and W. K. Kwok, Phys. Rev. Lett. **111**, 067001 (2013).
[13]J. Trastoy, M. Malnou, C. Ulysse, R. Bernard, N. Bergeal, G. Faini, J. Lesueur, J. Briatico, and J. E. Villegas, e-print arXiv:1307.2881.
[14]L. A. S. Mól, R. L. Silva, R. C. Silva, A. R. Pereira, W. A. Moura-Melo, and B. V. Costa, J. Appl. Phys. **106**, 063913 (2009).
[15]L. A. S. Mól, W. A. Moura-Melo, and A. R. Pereira, Phys. Rev. B **82**, 054434 (2010).
[16]R. C. Silva, F. S. Nascimento, L. A. S. Mól, W. A. Moura-Melo, and A. R. Pereira, New J. Phys. **14**, 015008 (2012).
[17]I. A. Ryzhkin, J. Exp. Theor. Phys. **101**, 481 (2005).
[18]C. Castelnovo, R. Moessner, and L. Sondhi, Nature **451**, 42 (2008).
[19]S. T. Bramwell, S. R. Giblin, S. Calder, R. Aldus, D. Prabhakaran, and T. Fennell, Nature **461**, 956 (2009).
[20]D. J. P. Morris, D. A. Tennant, S. A. Grigera, B. Klemke, C. Castelnovo, R. Moessner, C. Czternasty, M. Meissner, K. C. Rule, J.-U. Hoffmann, K. Kiefer, S. Gerischer, D. Slobinsky, and R. S. Perry, Science **326**, 411 (2009).
[21]H. Kadowaki, N. Doi, Y. Aoki, Y. Tabata, T. J. Sato, J. W. Lynn, K. Matsuhira, and Z. Hiroi, J. Phys. Soc. Jpn. **78**, 103706 (2009).
[22]Y. Nambu, Phys. Rev. D **10**, 4262 (1974).
[23]R. C. Silva, R. J. C. Lopes, L. A. S. Mól, W. A. Moura-Melo, G. M. Wysin, and A. R. Pereira, Phys. Rev. B **87**, 014414 (2013).
[24]J. P. Morgan, A. Stein, S. Langridge, and C. Marrows, Nat. Phys. **7**, 75 (2011).
[25]B. Van de Wiele, A. Manzin, A. Vansteenkiste, O. Bottauscio, L. Dupre, and D. De Zutter, J. Appl. Phys. **111**, 053915 (2012).
[26]D. H. Y. Tse, S. J. Steinmuller, T. Trypiniotis, D. Anderson, G. A. C. Jones, J. A. C. Bland, and C. H. W. Barnesh, Phys. Rev. B **79**, 054426 (2009).
[27]Y. Luo and V. Misra, Nanotechnology **17**, 4909–4911 (2006).
[28]L. Torres, L. Lopez-Diaz, O. Alejos, and J. Iniguez, Physica B **275**, 59 (2000).
[29]D. Weller and A. Moser, IEEE Trans. Magn. **35**, 4423 (1999).
[30]M. J. Donahue and D. G. Porter, *OOMMF v1.2a3 Object Oriented MicroMagnetic Framework, Software* (NIST, 2004).
[31]L. D. Landau and E. Lifshitz, Phys. Z. Sowjetunion **8**, 153 (1935).
[32]L. Gilbert, Phys. Rev. **100**, 1243 (1955).
[33]V. Bhat, J. Woods, L. E. De Long, J. T. Hastings, V. V. Metlushkoc, K. Rivkind, O. Heinonene, J. Sklenar, and J. B. Ketterson, Physica C **479**, 83–87 (2012).
[34]L. Sun, R. X. Cao, B. F. Miao, Z. Feng, B. You, D. Wu, W. Zhang, A. Hu, and H. F. Ding, Phys. Rev. Lett. **110**, 167201 (2013).
[35]T. Koyama, G. Yamada, H. Tanigawa, S. Kasai, N. Ohshima, S. Fukami, N. Ishiwata, Y. Nakatani, and T. Ono, Appl. Phys. Express **1**, 101303 (2008).
[36]S. Kasai, Y. Nakatani, K. Kobayashi, H. Kohno, and T. Ono, Phys. Rev. Lett. **97**, 107204 (2006).
[37]C. C. Wang, A. O. Adeyeye, and Y. H. Wu, J. Appl. Phys. **94**, 6644 (2003).